ELSEVIER

Coordination Chemistry Reviews 237 (2003) 147–161

COORDINATION CHEMISTRY REVIEWS

www.elsevier.com/locate/ccr

Structures and properties of multinuclear vanadium(III) complexes: seeking a clue to understand the role of vanadium(III) in ascidians

Kan Kanamori *

Department of Chemistry, Faculty of Science, Toyama University, Gofuku 3190, Toyama 930-8555, Japan

Received 25 January 2002; accepted 20 September 2002

Contents

Abstract

Certain ascidians accumulate vanadium(III) to a great extent in their blood cells. The role of vanadium(III) in ascidians is still a controversial issue, though 90 years have already passed since the original finding by Henze was published. In order to obtain further insight into the role of vanadium(III) in ascidian blood cells, the coordination chemistry of vanadium(III) has been developed. This review will survey (1) the vanadium(III) complexes bridged by a single oxo group, focusing on the relationship between the preferential formation of μ-oxo dimers and chemical properties of vanadium(III) complexes; (2) the vanadium(III) complexes containing ligands with a terminal alkoxo functionality; (3) the vanadium(III) complexes with dinucleating ligands, which exhibit diverse bridging modes; (4) the sulfato-containing vanadium(III) complexes with regard to the role of sulfate ions in ascidian blood cells; (5) the multinuclear vanadium(III) complexes with various bridging modes and (6) the magnetic coupling of dinuclear vanadium(III) complexes.

Keywords: Vanadium(III) complexes; Oxo bridge; Alkoxo bridge; Dinucleating ligands; Sulfato complexes

1. Introduction

Henze's discovery that certain ascidians (tunicates) sequester vanadium(III) in their blood cells spurred the interest of chemists in vanadium(III) complexes [1]. *Ascidia gemmata* contains as high as 0.35 M vanadium in its blood cells, which corresponds to 10^7 times the vanadium concentration in seawater [2]. It has also been known that a considerable amount of sulfate coexists with vanadium(III) in the blood cells of ascidians [3]. The fan worm, *Pseudopotamilla occelata*, was found to be the second vanadium(III) accumulator in the animal kingdom [4].

* Tel.: +81-76-445-6609; fax: +81-76-445-6549
E-mail address: kanamori@sci.toyama-u.ac.jp (K. Kanamori).

0010-8545/02/$ - see front matter
PII: S0010-8545(02)00279-5

Although many chemists as well as biologists have long made efforts to reveal the role of vanadium(III) in ascidians, the physiological function still remains unclear. Several potential roles of vanadium in ascidians have been reviewed, which include mediation of the assimilation of sulfur dioxide, protection from microbes or other predators, histoincompatibility responses, peroxide production/sterilization, and tunic biogenesis [5]. Although there are views that vanadium(III) in ascidians may perhaps represent a metabolic terminus [5] and that vanadium(III) itself may not play any important role in its physiology [6], a view that vanadium(III) itself may play an important role in ascidians is taken in this review. Generally, inorganic chemists prepare model compounds mimicking the structure of metal compounds in biological systems and elucidate those properties to approach the point of the structure–function relationship of the metal compounds in life. Due to the aforementioned situation of the studies of vanadium(III) in ascidians, model studies cannot be performed at present. However, the study of the structures and properties of vanadium(III) compounds with biologically relevant ligands may give a clue to understand the puzzling role of vanadium(III) in ascidians.

Di- or multinuclear iron and manganese complexes play important roles in biochemical reactions [7]. For example, oxo-bridged dinuclear iron(III) species have been found in the invertebrate dioxygen carrier, hemerythrin, and in the enzymes ribonuclease reductase, purple acid phosphatase, and methane monooxygenase. Dinuclear manganese complexes have also been investigated with regard to the metal center of photosystem II (PSII) in green plants. Considering these facts, it is not unreasonable to speculate that di- or multinuclear vanadium(III) species may be a plausible active form of vanadium(III) in vanadium-accumulating animals.

The green monomeric aquavanadium(III) ion is easily hydrolyzed to form a brown species. An intense absorption band appears at ca. 420 nm upon hydrolysis. Boeri and Ehrenberg have observed a similar phenomenon for vanadocyte hemolysate, so-called Henze's solution, from *Ascidia obliqua* [8]. Pajdowski has assigned the intense absorption band due to the brown species to a charge-transfer transition of the dinuclear vanadium(III) complex with a di(μ-hydroxo) bridge [9]. Newton and Baker, on the other hand, have defined the brown species to be an oxo-bridged dinuclear vanadium(III) complex [10]. Several oxo-bridged dinuclear vanadium(III) complexes have been characterized by 1990 by X-ray crystallography, including $[V_2OCl_4(THF)_6]$ [11], $[V_2O(SCH_2CH_2NMe_2)_4]$ [12], $[V_2O(bpy)_2Cl_2]Cl_2\cdot 6H_2O$ [13], $[V_2OCl_4(py)_6]$ [14], and $[V_2O(Me_3tacn)_2(acac)_2]I_2\cdot 2H_2O$ (Me_3tacn: 1,4,7-trimethyl-1,4,7-triazacyclononane) [15]. Although the above ligand sets yield the μ-oxo dimer, the vanadium(III) complexes with some other types of ligands do not yield the μ-oxo dimer at all. Furthermore, *N*-(2-hydroxyethyl)ethylenediamine-*N*,*N*′,*N*′-triacetate (hedta) has been known to form a di(μ-alkoxo)-bridged dinuclear vanadium(III) complex [16]. It is, therefore, of interest to examine what kind of di- or multinuclear vanadium(III) complexes can be obtained depending on the specific characteristics of ancillary ligands.

2. Vanadium(III) complexes with a single oxo bridge

2.1. Vanadium(III) species in Henze's solution

Boeri and Ehrenberg have shown that Henze's solution from *Ascidia obliqua* becomes dark brown above pH 2, concurrent with the appearance of the intense absorption band at ca. 420 nm [8]. Identical spectral changes have been observed for the solution of a simple vanadium(III) salt, indicating that the same species as in Henze's solution must be present in this solution. The brown species that is responsible for the intense absorption band at ca. 420 nm has been characterized using the resonance Raman spectra of aqueous $V_2(SO_4)_3$ solution [17]. Fig. 1 shows the pH dependence of the visible absorption spectra of aqueous $V_2(SO_4)_3$ solution.

The intensities of three Raman bands were enhanced upon resonance with the intense absorption band at ca. 420 nm. Fig. 2 shows the resonance Raman spectra excited with 514.5 nm (Ar^+ ion laser) as a function of pH. The Raman bands observed at pH 0.4 can be assigned to SO_4^{2-}, HSO_4^-, $V(H_2O)_6^{3+}$, and H_2O. The most intense band at 987 cm^{-1} is due to $\nu_s(SO_4)$ and can be used as an intensity standard. The new Raman bands appeared at 1533 and 774 cm^{-1} at pH 1.3. The intensities of these bands increased with increasing pH of the solution. It can be recognized that these bands were strongly enhanced at pH 2.4 by comparing the intensities of the bands with that of the sulfate band at 987 cm^{-1}. A third new band was detected at ca. 480 cm^{-1} at pH 2.4. These three Raman bands can be

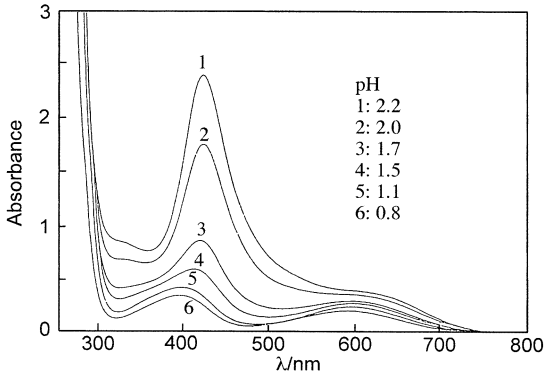

Fig. 1. pH dependence of the absorption spectrum of $V_2(SO_4)_3$ (40 mM/V(III) atom) [17].

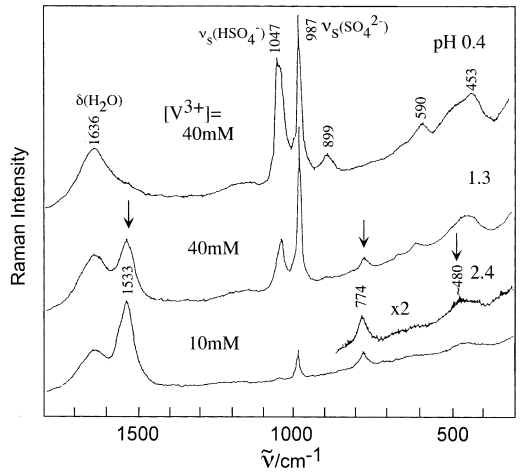

Fig. 2. Raman spectra (514.5-nm excitation) of aqueous $V_2(SO_4)_3$ as a function of pH [17].

assigned to the vibrations of the brown species formed in the higher pH solution.

Two alternative structures have been proposed for the brown species (Scheme 1), di(μ-hydroxo) [9] and μ-oxo [10]. Whether the brown species has a di(μ-hydroxo) or μ-oxo structure can be determined using a 1:1 isotopic mixture of $H_2^{16}O$ and $H_2^{18}O$. If the brown species adopts the di(μ-hydroxo) structure, three isotopic species, $V(^{16}OH)_2V$, $V(^{16}OH)(^{18}OH)V$, and $V(^{18}OH)_2V$, will be present in the solution in a ratio of 1:2:1. On the other hand, if the brown complex is the μ-oxo dimer, only two species, $V-^{16}O-V$ and $V-^{18}O-V$, will be present in a 1:1 ratio.

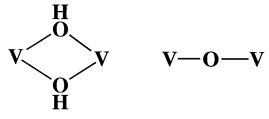

di(μ-hydroxo) μ-oxo

Scheme 1.

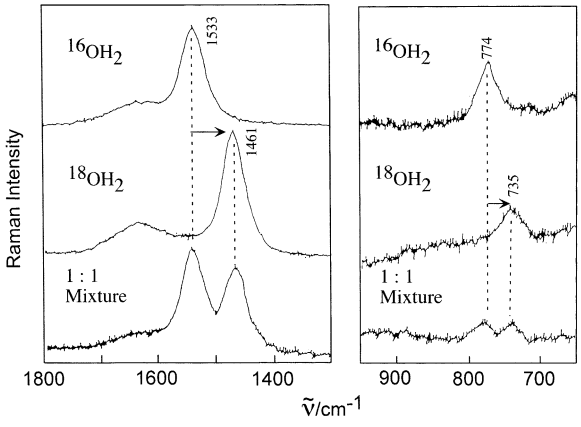

Fig. 3. Raman spectra of VCl_3 in $H_2^{16}O$, $H_2^{18}O$, and 1:1 mixture of $H_2^{16}O/H_2^{18}O$ at pH 2 [17].

Fig. 3 shows the resonance Raman spectra of the brown species obtained in normal water, in $H_2^{18}O$, and in the 1:1 $H_2^{16}O$:$H_2^{18}O$ mixture. The 1533- and 774-cm^{-1} bands shifted to lower wave numbers when $H_2^{18}O$ was used as a solvent. This observation allows assignment of the vibrations in which the oxygen atom participates. In the 1:1 mixture, only two bands were observed at the positions corresponding to the isotopically pure species, indicating that the brown species is the μ-oxo dimer and not the di(μ-hydroxo) dimer.

The resonance-enhanced Raman bands at 1533, 774, and ca. 480 cm^{-1} can be assigned to the first overtone of V–O–V antisymmetric stretching ($2 \times \nu_{as}$(V–O–V)), the V–O–V antisymmetric stretching (ν_{as}(V–O–V)), and the V–O–V symmetric stretching (ν_s(V–O–V)), respectively. The CT transition and the resonance-enhanced Raman bands are very useful to detect μ-oxo dimer of vanadium(III) formed in the solution. Especially, $2 \times \nu_{as}$(V–O–V) mode is diagnostic since it appears as a very intense and broad band in the region where the intraligand vibrations are less overlapping. Other examples of the Raman spectra where $2 \times \nu_{as}$(M–O–M) mode was observed as a more intense band than the fundamental have been reported for the iron(III) complex [18] and the Mo(V) complex [19]. This interesting characteristic is discussed based on the symmetry consideration of the vibrational modes [19,20]. In C_i symmetry for a dinuclear complex with a linear M–O–M, a fundamental ν_{as}(M–O–M) mode is Raman-forbidden, while its overtone become Raman-allowed [19]. Under the C_{2v} symmetry of the bent M–O–M bridge, the fundamental is of B_2 symmetry and requires a vibronic mechanism for activation, which is generally much weaker than a Frank–Condon A-term mechanism, whereas its overtone is of A_1 symmetry and is Frank–Condon allowed [20].

2.2. Vanadium(III) complexes containing aminopolycarboxylates

It has been known that a decadentate aminopolycarboxylate ligand triethylenetetramine-*N*,*N*,*N*′,*N*″,*N*‴,*N*‴-hexaacetate (ttha) forms a μ-oxo dinuclear vanadium(III) complex which exhibits a characteristic visible absorption band similar to that observed for the aqua species [21]. On the contrary, the vanadium(III)–edta complex shows an absorption profile distinctly different from that of the ttha complex, and does not exhibit the characteristic absorption band due to the V–O–V moiety upon alkaline hydrolysis [22]. It is, therefore, of interest to determine which types of vanadium(III) complexes yield the μ-oxo dimer and which types do not. The properties of the solution of (aminopolycarboxylato)vanadium(III) complexes have been systematically examined with this in mind [23].

The aminopolycarboxylate ligands examined are listed in Scheme 2. Typical examples in which different absorption profiles were observed upon alkaline hydrolysis are shown in Figs. 4 and 5. Although hexadentate ligands, edds and edta have the same donor set, N_2O_4, the hydrolytic behavior of the edds and edta complexes is different. The vanadium(III) complex with edds exhibits a very intense absorption band at high pH values, indicating that the μ-oxo dimer is formed upon alkaline hydrolysis. In contrast, the edta complex does not show an intense CT band due to the V–O–V moiety even at high pH values, indicating that the μ-oxo dimer is not formed with edta. A similar difference in hydrolytic behavior was observed for the vanadium(III) complexes with β-alada and nta (Fig. 5), both of which have a NO_3 donor set. Two Raman spectra of solutions of the edds complex are shown in Fig. 6. The Raman spectrum observed at pH 8.20 is completely different

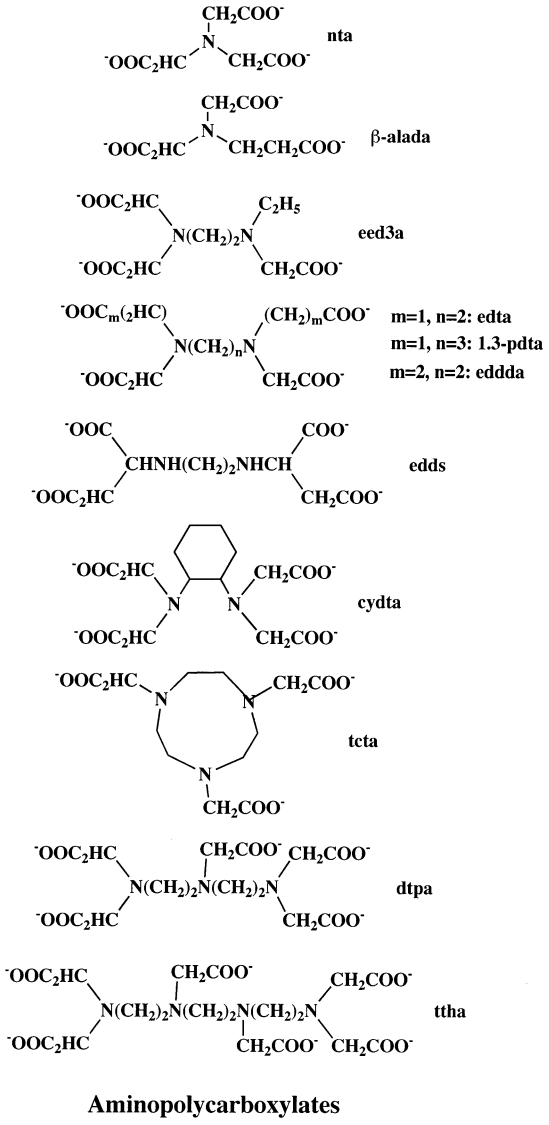

Scheme 2.

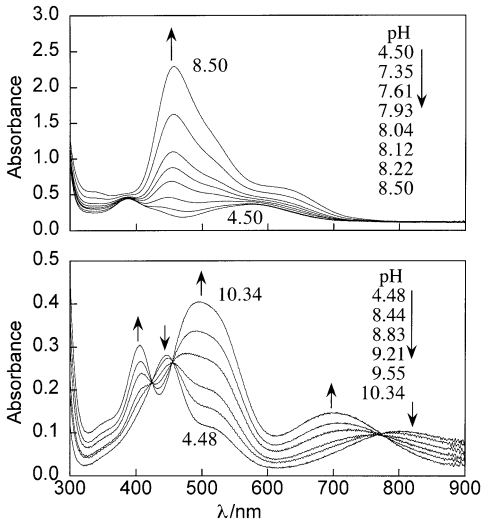

Fig. 4. Absorption spectra of K[V(III)(*S*,*S*′-edds)]·H_2O (8.63 mM) (upper) and K[V(III)(edta)(H_2O)]·$2H_2O$ (10.24 mM) (lower) as a function of pH [23].

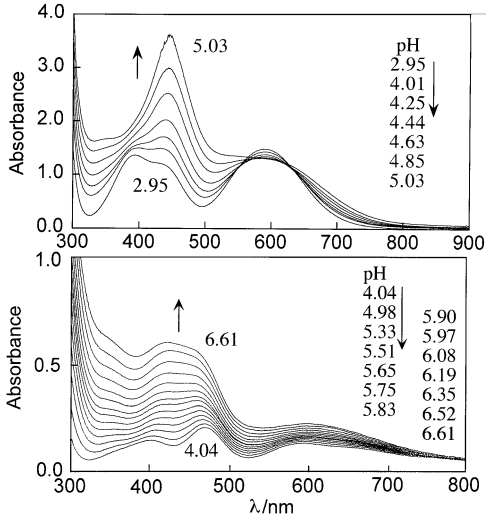

Fig. 5. Absorption spectra of [V(III)(β-alada)(H_2O)$_2$] (49.9 mM) (upper) and K[V(III)(edta)(H_2O)]·$2H_2O$ (10.24 mM) (lower) as a function of pH [23].

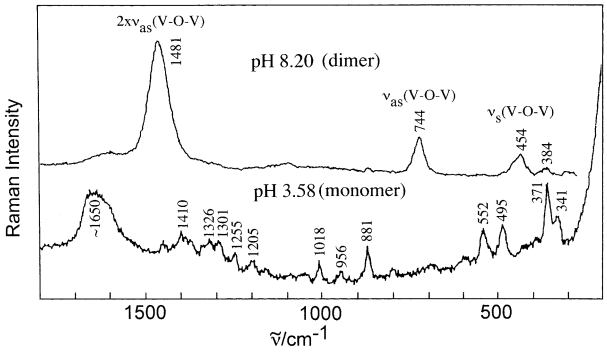

Fig. 6. Raman spectra of [V(III)(*S*,*S*′-edds)]$^-$ in aqueous solution.

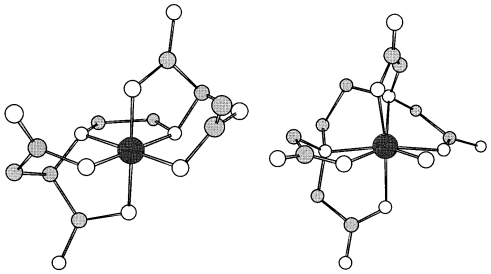

(A) (B)

Fig. 7. Structures of $[V(III)(S,S'\text{-edds})]^-$ (A) [23] and $[V(III)(edta)(H_2O)]^-$ (B) [24].

from that observed at pH 3.58, and is dominated by the resonance-enhanced bands due to the V–O–V moiety, as in the case of the aqua species.

The structure of the parent monomeric complex can account for why the edds and β-alada complexes yield the μ-oxo dimer while the edta and nta complexes do not. Fig. 7 shows the structures of the edds [23] and the edta [24] complexes. The edta complex adopts a heptacoordinate structure described as a capped trigonal prism and contains an additional water molecule along with a hexadentate edta ligand. On the other hand, the edds complex adopts an octahedral structure without an additional water molecule. Fig. 8 shows the structures of the vanadium(III) complexes with β-alada [25] and nta [26]. The nta complex adopts a capped octahedral heptacoordinate structure with a quadridentate nta ligand and three aqua ligands. The β-alada complex, on the other hand, adopts a hexacoordinate structure with a quadridentate β-alada ligand and two aqua ligands. The heptacoordination of the edta and nta vanadium(III) complexes is considered to be a result of the small chelate-ring size of edta and nta, which is not large enough to encircle the vanadium(III) ion. While edta and nta only form five-membered chelate rings, edds and β-alada form two and one six-membered chelate rings, respectively. Normal hexacoordinate structures found in the edds and β-alada complexes have been explained to be a result of the increase in the chelate-ring size.

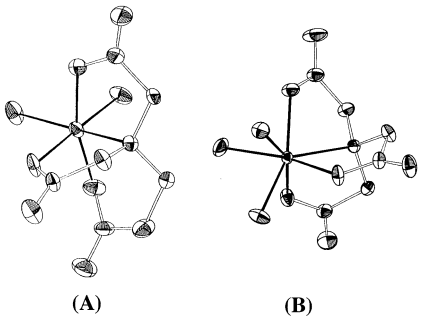

(A) (B)

Fig. 8. Structures of $[V(III)(\beta\text{-alada})(H_2O)_2]$ (A) [25] and $[V(III)(nta)(H_2O)_3]$ (B) [26].

In order to determine whether or not a correlation really exists between the coordination number and the dimerization tendency for vanadium(III) complexes with aminopolycarboxylate ligands, the structures of vanadium(III) complexes with other aminopolycarboxylate ligands were examined. The 1,3-pdta [27] and eddda [25] vanadium(III) complexes have been characterized, based on X-ray crystallography, to have a hexacoordinate structure. On the other hand, the cydta vanadium(III) complex adopts a heptacoordinate structure [28]. The structures of the tcta, dtpa, and eed3a complexes have been estimated based on the visible spectral characteristics [27] and ^{1}H-NMR spin-lattice relaxation time [23] since these complexes did not yield a sufficient quality of crystals for X-ray analysis.

Aminopolycarboxylate ligands can be classified into two categories according to the hydrolytic behavior of their vanadium(III) complexes.

category I: ttha, 1,3-pdta, edds, eddda, eed3a, β-alada
category II: edta, cydta, dtpa, tcta, nta

All of the vanadium(III) complexes with a category I ligand adopt a hexacoordination and always yield the μ-oxo dimer upon alkaline hydrolysis, while the vanadium(III) complexes with a category II ligand adopt a heptacoordination and do not form the μ-oxo dimer at all. Thus, the coordination number of the parent monomer is a factor that dominates the formation of the μ-oxo dimer of aminopolycarboxylato vanadium(III) complexes. The ligands in category II form only five-membered chelate rings, while the category I ligands form at least one six-membered chelate ring, except ttha and eed3a. Thus, it can be concluded that the chelate-ring size plays an important role in determining the coordination number of the vanadium(III) complexes with aminopolycarboxylate ligands.

The difference in the hydrolytic behavior between the hexa- and heptacoordinate species has been interpreted by assuming a putative intermediate, a di(μ-hydroxo) species, in the oxo-bridged dimer formation [23].

$$[VL]^{n-} + H_2O \rightleftharpoons [VL(OH)]^{(n+1)-} + H^+$$

$$2[VL(OH)]^{(n+1)-} \rightleftharpoons [V_2L_2(\mu\text{-}OH)_2]^{2(n+1)-}$$

$$[V_2L_2(\mu\text{-}OH)_2]^{2(n+1)-} \rightleftharpoons [V_2L_2(\mu\text{-}O)]^{2(n+1)-} + H_2O$$

If the dihydroxo-bridged intermediate is formed by the association of two hydroxo species, the coordination number increases in this step. If the monomer contains heptacoordinate vanadium(III), the intermediate must contain octacoordinate vanadium(III), which is highly unfavorable for vanadium(III) complexes. As a result, the heptacoordinate vanadium(III) monomeric complex does not form the μ-oxo dimer upon base hydrolysis. $[V_2O(BH_4)_4(PMe_3)_4]$ is the only exception of the above hypothesis, since the vanadium(III) atom in this com-

plex adopts a heptacoordination [29]. The small bite angles of BH_4 chelate (55–60°) would make it possible to form the heptacoordinated μ-oxo dimer.

Interestingly, although $[V(III)(tmdta)]^-$ (tmdta: tetramethylenediamine-*N*,*N*,*N*′,*N*′-tetraacetate) adopts a hexacoordinate structure, it does not form a μ-oxo dimer in the higher pH region [30]. The failure to form a μ-oxo dimer is considered to be due to the instability of the seven-membered chelate ring.

2.3. Vanadium(III) complexes containing tripodal quadridentate ligands with pyridyl groups

The formation of the μ-oxo dimer depends not only on the chelate ring size but also on the specific functional group [31]. Therefore, it has been examined whether or not the replacement of an acetate group of nta by a methylpyridyl group would change the preferences of oxo-bridged dimers. The pyridyl-containing ligands, pda, bpg, and tpa, only form five-membered chelate rings, similar to nta (Scheme 3). It is thus expected that these ligands would fail to generate the μ-oxo dimer. However, this expectation was not fulfilled.

Fig. 9 shows a perspective view of the vanadium(III)–tpa complex. The complex is an oxo-bridged dinuclear vanadium(III) complex with a slightly bent V–O–V moiety (175.3(2)°). The monomeric unit adopts hexacoordination, although the coordination polyhedron around the vanadium(III) center is significantly distorted from a regular octahedron because of the restricted bite angles of the tpa ligand (*cis* N–V–N′ angle range is 77.0(1)–91.2(1)° and *trans* N–V–N angles are 157.8(1) and 157.5(1)°).

Although crystals of the bpg and pda complexes could not be obtained, the structures of the complexes were determined based on the visible absorption and resonance Raman spectra. Fig. 10 shows the pH-dependent visible absorption spectra of $[V(III)(pda)(OH)(OH_2)]$ and the resonance Raman spectrum of $[V_2O(pda)_2(H_2O)_2]$. The intense LMCT band observed at

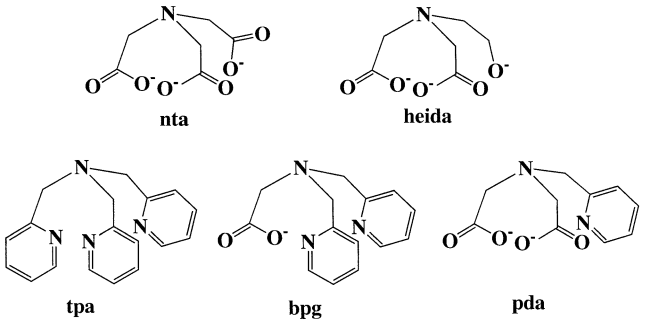

Scheme 3.

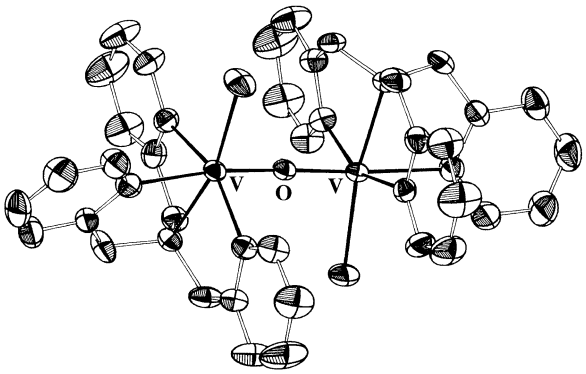

Fig. 9. Structure of $[V(III)_2OBr_2(tpa)_2]^{2+}$ [31].

higher pH values and the characteristic Raman bands indicate that pda also forms a μ-oxo dimeric complex. Similar diagnostic visible and Raman bands were observed for the bpg–vanadium(III) complex. Therefore, replacement of an acetate group of nta by a pyridylmethyl group results in a hexacoordinate species regardless of the number of pyridylmethyl groups, and as a result, generates a μ-oxo dimer.

Contrary to the tripodal quadridentate ligand, bpedda (*N*,*N*′-bis(2-pyridylmethyl)-1,2-ethanediamine-*N*,*N*′-diacetate), where two acetate groups of a hexadentate ligand, edta, are replaced by two pyridylmethyl groups, yields the heptacoordinate structure and does not generate a μ-oxo dimer [30]. However, bppdda (*N*,*N*′-bis(2-pyridylmethyl)-1,3-propanediamine-*N*,*N*′-diacetate), which forms a six-membered chelate ring, generates the μ-oxo dimer as in the case of 1,3-pdta.

The μ-oxo dimer can also be obtained by using an amino acid ligand, histidine. Fig. 11 depicts the structure of $[V(III)_2O(L\text{-}his)_4]$ [32]. In this complex, one histidine coordinates to the vanadium(III) center in a tridentate fashion, and the other one in a bidentate fashion. It is interesting that the hard vanadium atom prefers a soft imidazole nitrogen rather than a hard carboxylate oxygen in this complex. Czernuszewicz et al. redetermined the structure of $[V(III)_2O(L\text{-}his)_4]$ using a different space group (*C*2) from the original one (*P*1). They have shown that the bent V–O–V moiety in the solid state is due to the hydrogen bond between the monomeric units and that the V–O–V angle opens up to ca. 180° upon dissolution due to a breaking of the hydrogen bond [33]. The speciation of the vanadium(III)–histidine system in aqueous solution has been studied [34], showing that $[V(III)_2O(L\text{-}his)_4]$ species predominantly exists in solution at pH 6–8.5 range.

At this point, it is appropriate to mention the structure of the V–O–V dimer in the CT excited state deduced from the resonance Raman characteristics of the V(III)–O–V(III) dimeric compounds. In general, the symmetric M–O–M stretching is a dominant mode and the antisymmetric M–O–M stretching is usually weak

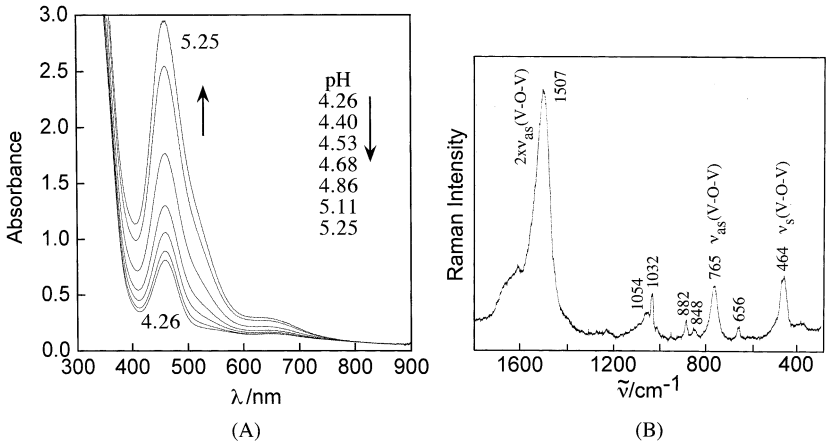

Fig. 10. (A): Absorption spectra of [V(III)(pda)(OH)(H_2O)] (18 mM) in aqueous solution as a function of pH and (B): Raman spectrum of [$V(III)_2O(pda)_2(H_2O)_2$] in the solid state.

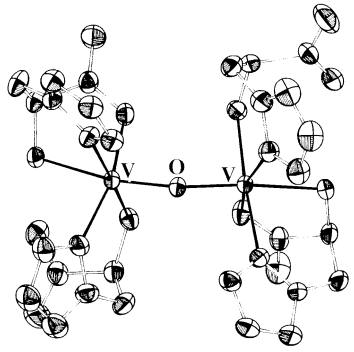

Fig. 11. Structure of [$V(III)_2O$(L-his)$_4$] [32].

or not observed in the resonance Raman spectra of the oxo-bridged dinuclear metal complexes [35]. In the above cases, however, the antisymmetric stretching is sometimes stronger than the symmetric one and the first overtone of the antisymmetric stretching is dominant. These resonance Raman characteristics of the μ-oxo dimer of vanadium(III) should reflect the geometry of the bridging moiety in the charge-transfer (CT) excited state; the equilibrium conformation of the molecule is distorted along the normal coordinate for the Raman band that is resonance-enhanced in the transition from the ground state to the excited state [36]. Thus, it is considered that the bridging moiety of the oxo-bridged vanadium(III) complexes that have the above characteristics is antisymmetrically distorted in the CT excited state, namely, of the V^{4+}=O–V^{2+} type [20,23].

Further examples of dinuclear vanadium(III) complexes with a single oxo bridge have been reported recently, including $[V_2OCl_2(phen)_4]^{2+}$ [37], $[V_2O(NH_3)_{10}]^{4+}$ [38], and $[V_2OCl_2(bis\text{-}bpy)_2]^{2+}$ (bis-bpy: 1,2-bis(2,2′-bipyridyl-6-yl)ethane) [39]. Carrano et al. have reported an interesting biological reaction with single oxo-bridged vanadium(III) complexes; i.e. $[V_2OL_4Cl_2]^{2+}$-type complexes (L = 2,2′-bipyridine, 1,10-phenanthroline, or its derivatives) interact very strongly with DNA and lead to its degradation [37]. Whether this finding is relevant to the vanadium(III) in ascidians or not, it is worth noting that the oxo-bridged dinuclear vanadium(III) compounds exhibit a biological function.

In conclusion, the factors affecting the formation of the μ-oxo dimer are not only the chelate-ring size but also the ligand structure and the specific functional group.

2.4. Correlation between ν_{as}(V–O–V) and the LMCT maxima

A good positive linear correlation was observed between $2 \times \nu_{as}$(V–O–V) and the LMCT maxima, as shown in Fig. 12. Generally the energy of the M–O–M stretching vibration depends on both the M–O–M angle and the force constant of the M–μ-O bond [33,35,40]. The effect due to the difference in the V–O–V angles, however, is considered negligible in vanadium(III) complexes with a single oxo bridge [31] though there may be some exception such as [$V(III)_2O$(L-his)$_4$] [32,33]. In Fig. 12, it appears that the greater the softness of the ancillary ligands, the lower the energies of V–O–V stretching and LMCT transition. The covalency (including π-bonding) of the V(III)–μ-O bond is expected to be reduced by a soft ancillary ligand based on the argument presented by Reem et al. [41]. The decrease in the π-bonding character results in a redshift of the LMCT transition as well as a decrease in the force constant of the V(III)–μ-O stretching vibration. Thus, a positive correlation found between the energy of the LMCT transition and ν_{as}(V–O–V) would be useful for estimating the coordination environment of an unknown species with a μ-oxo bridge in solution.

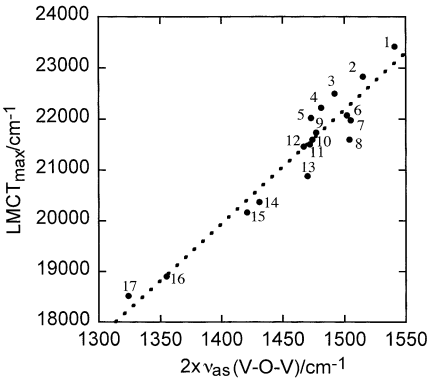

Fig. 12. Correlation between $2 \times \nu_{as}$(V–O–V) and the LMCT maxima: 1, aqua complex in solution; 2, edda complex in solution; 3, β-alada complex in solution; 4, edds complex in solution; 5, nitriloacetatedipropionate complex in solution; 6, ttha complex in solution; 7, eed3a complex in solution; 8, pda complex in the solid state; 9, eddda complex in solution; 10, 1,3-pdta complex in solution; 11, tris(2-pyridylmethyl)-1,4,7-triazacyclononane complex in solution; 12, 1,3-propanediamine-*N*,*N*′-disuccinate complex in the solid state; 13, bpg complex in the solid state; 14, L-his complex in the solid state; 15, bispicen complex in solution; 16, bpg complex in the solid state; 17, tpa complex in the solid state [31].

Dependence of charge-transfer transition energy upon redox potentials has been discussed [42]. It was anticipated that as the oxidation potential of the metal complex increases, LMCT transition should move to lower energy. Thus, a study of the oxidation potentials of oxo-bridged dinuclear vanadium(III) complexes should be an interesting subject in future.

3. Vanadium(III) complexes bridged by a terminal alkoxo group

The structures of vanadium(III) complexes containing a ligand with a terminal alkoxo group have been examined. Ligands heida (Scheme 3) and hedta (*N*-hydroxyethylethylenediamine-*N*,*N*′,*N*′-triacetate) have structures closely related to those of nta and edta, respectively. These ligands also form only five-membered chelate rings upon coordination, similar to nta and edta. The structural preferences in vanadium(III) complexes containing these ligands were further explored.

Fig. 13A shows the structure of the heida–vanadium(III) complex [43] and Fig. 13B that of the hedta–vanadium(III) complex [16]. Both complexes contain a di-μ-alkoxo bridge derived from the deprotonation of the hydroxyethyl group. The vanadium(III) center of the heida complex adopts a hexacoordination in spite of the fact that the meridional coordination of the iminodiacetate moiety leads to a large distortion in the axial O–V–O angle (149.49(7)°), while that of the hedta complex adopts heptacoordination. Therefore, these observations indicate that the coordination geometry of vanadium(III) complexes can be flexibly changed depending on the ligand structure.

4. Vanadium(III) complexes containing a dinucleating ligand

Several dinucleating ligands are shown in Scheme 4. The central alkoxo group in the ligands is expected to serve as a bridging group. It has been shown that different functionalities of the ligands result in various kinds of vanadium(III) complexes in which not only the coordination numbers but also the bridging mode vary.

Two vanadium(III) complexes with different bridging modes have been obtained using dpot. Fig. 14 shows a perspective view of $[V_2(dpot)_2]^{2-}$ [27]. The two vanadium(III) centers are linked by two central alkoxo groups of two dpot ligands, forming a rhombic V_2O_2 core, as found in $[V(III)_2(heida)_2(H_2O)_2]$ [43] and $[V(III)_2(hedta)_2]^{2-}$ [16]. Each vanadium(III) center adopts a distorted pentagonal–bipyramidal structure with heptacoordination.

A dinuclear vanadium(III) complex, which is different from the 2:2 dimer prepared by Robles, has been prepared using the same ligand dpot in the presence of benzoate [44,45]. Fig. 15 shows a perspective view of

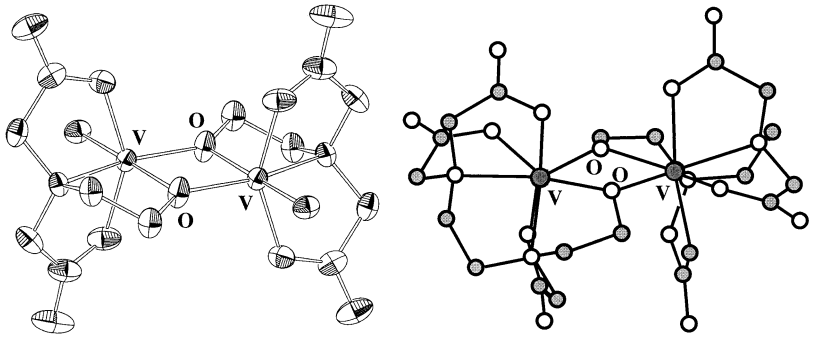

Fig. 13. Structures of $[V(III)_2(heida)_2(H_2O)_2]$ (A) [43] and $[V(III)_2(hedta)_2]^{2-}$ (B) [16].

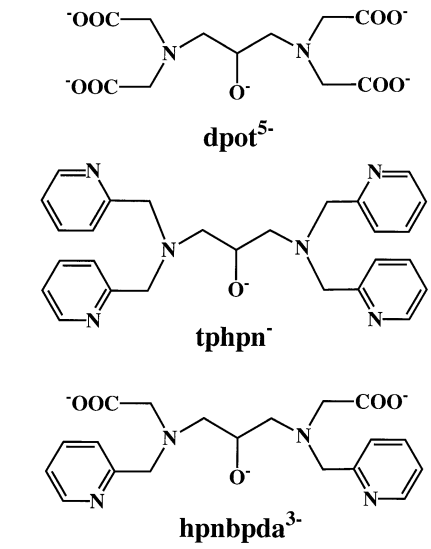

Scheme 4.

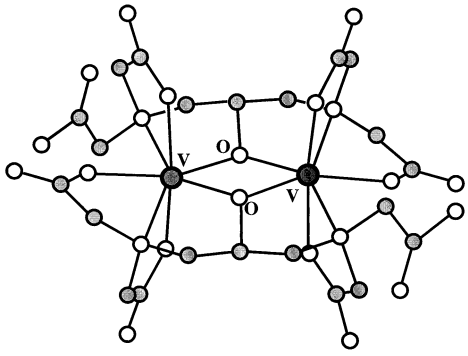

Fig. 14. Structure of $[V(III)_2(dpot)_2]^{2-}$ [17].

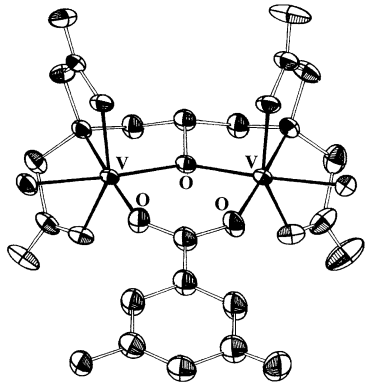

Fig. 15. Structure of $[V(III)_2(dpot)(m\text{-hbza})(H_2O)_2]$ [44,45].

$[V_2(dpot)(m\text{-hbza})(H_2O)_2]$ (*m*-hbza: *m*-hydroxybenzoate). In contrast to the heptacoordination in $[V_2(dpot)_2]^{2-}$, each vanadium(III) center in the complex adopts a hexacoordinate structure. This difference in the coordination number may result from the expansion of the bridging core induced by the carboxylato bridge. Interestingly, the two carboxylato groups are in *cis* positions in $[V_2(dpot)_2]^{2-}$, while they occupy *trans* positions in $[V_2(dpot)(m\text{-hbza})(H_2O)_2]$ regardless of a large distortion in the octahedron.

A dinucleating ligand, tphpn, has four pyridylmethyl groups in place of four acetate groups in dpot. Despite the fact that the tphpn–vanadium(III) complex was prepared in the same ternary system as the dpot complex, namely, V(III):dinucleating ligand:bza = 2:1:1, the bridging mode of the tphpn–vanadium(III) complex is different from that of the dpot system, as shown in Fig. 16 [45,46]. Two vanadium(III) centers are triply bridged by an alkoxo group of tphpn, a carboxylato group of bza, and an additional hydroxo group. As a consequence, each vanadium(III) center adopts heptacoordination, which differs from the dpot counterpart. Furthermore, unlike dpot, a 2:2 complex was not obtained with tphpn. The different coordination behavior of dpot and tphpn was interpreted in terms of the different charges of the ligands. Namely, a 2:2 complex with tphpn must have a high positive charge, +4, which would not be favorable.

The type of dinuclear vanadium(III) complexes which may be obtained using hpnbpda which has an intermediate structure between those of dpot and tphpn has been examined. The bis(hpnbpda)divanadium(III) complex has a structure similar to that of the bis(dpot) complex (Fig. 17) [45] with a heptacoordinate structure. The hpnbpda ligand acts as a heptadentate ligand, leaving one 2-methylpyridyl group free from coordination. This selection is reasonable since a hard vanadium(III) atom prefers a hard carboxylate oxygen atom over a soft pyridyl nitrogen atom. Di- and tetranuclear hpnbpda–vanadium(III) complexes with a bridging sulfato group have been prepared and characterized by X-ray crystallography [47].

The versatile structures of the vanadium(III) complexes formed by the dinucleating ligands again indicate

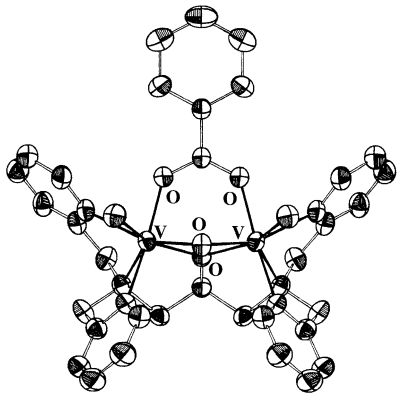

Fig. 16. Structure of $[V(III)_2(bza)(OH)(tphpn)(H_2O)_2]^{3+}$ [45,46].

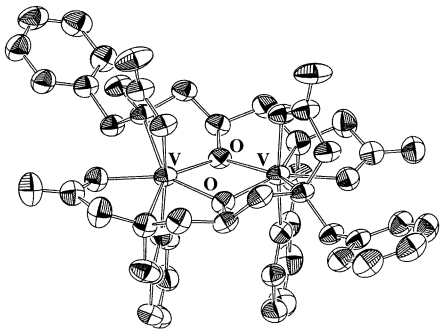

Fig. 17. Structure of $[V(III)_2(hpnbpda)_2]$ [45].

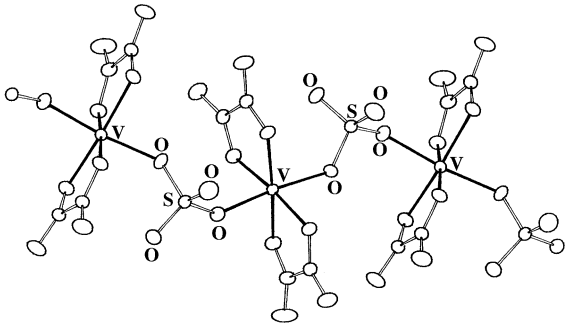

Fig. 18. Structure of $[V(III)(ox)_2(SO_4)]$ [49].

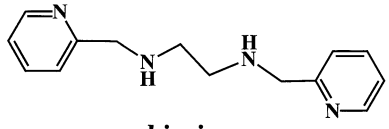

bispicen

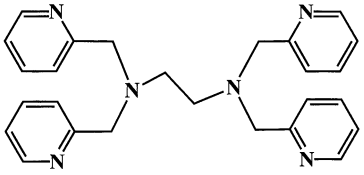

tpen

Ligands with Pyridyl Functionalities

Scheme 5.

the flexibility of the coordination geometry of vanadium(III) complexes.

5. Vanadium(III) complexes with a sulfato group

It is well known that the vanadium-containing blood cells of ascidians, so-called vanadocytes, also contain a large amount of sulfate [1,3]. With regard to the possible roles of such sulfate, Frank et al. hypothesized that complexation between vanadium(III) and the sulfate ion can lower the ionic strength at a high intracellular vanadium(III) concentration [48]. Therefore, it is of importance to explore the coordination chemistry of vanadium(III) complexes containing sulfate ions.

A linear polymeric vanadium(III) complex containing a sulfate ion was obtained. Fig. 18 shows the structure of $[V(III)(ox)_2(\mu\text{-}SO_4)]^{3-}$ [49]. The sulfate ion acts as a bidentate bridging ligand in this complex. The sulfate bridge in this complex is very unstable, and almost completely dissociates in an aqueous solution to give monomeric species. However, Raman spectroscopy reveals that a small portion of the vanadium(III) ions still maintains a direct bond with sulfate in an aqueous solution of $[V(III)(ox)_2(\mu\text{-}SO_4)]^{3-}$.

More stable vanadium(III) complexes with sulfate have been prepared using bispicen and tpen containing pyridyl functionalities (Scheme 5) [50]. A perspective view of $[V_2(SO_4)_3(bispicen)_2]$ is shown in Fig. 19. The monomeric unit is shown on the left side (A) and the dimeric unit on the right side (B), where the bispicen ligands are omitted for clarity. This complex contains two types of sulfate. One acts as a bidentate bridging ligand, and the other acts as a bidentate chelate ligand. The vanadium(III) center adopts a heptacoordinate structure that is induced by the bidentate coordination of sulfate. The properties of the solution of bispicen complex were examined. Fig. 20A shows the diffuse reflectance spectrum of the powder sample and the absorption spectrum of the aqueous solution. The

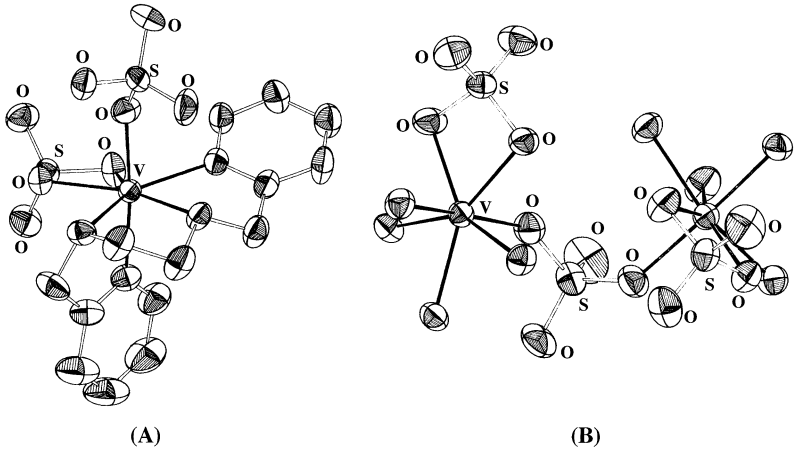

(A) (B)

Fig. 19. Structures of $[V(III)_2(SO_4)_3(bispicen)_2]$: (A) monomeric unit; (B) bridging moiety [50].

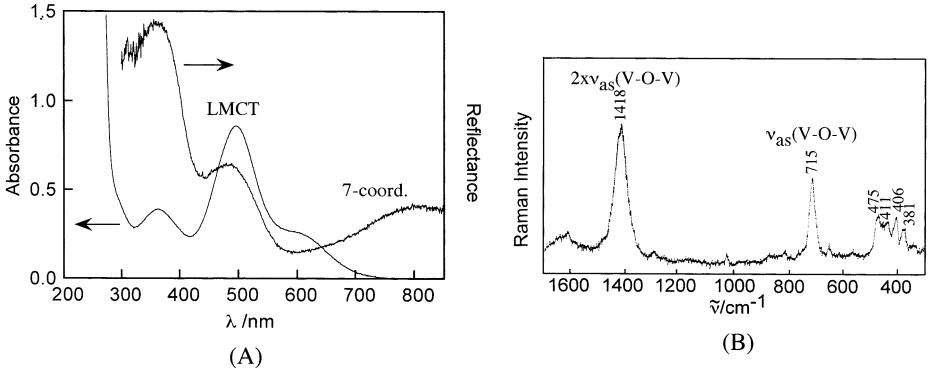

Fig. 20. (A): Absorption (2 mM, pH 3.25) and diffuse reflectance spectra and (B): Raman spectrum of the aqueous solution (0.85 mM, pH 3.5) of $[V(III)_2(SO_4)_3(bispicen)_2]$ [50].

reflectance spectrum exhibits a band at 800 nm, which is characteristic of the heptacoordinate vanadium(III) complex [23,27]. The heptacoordinate structure was found to be preserved in 99% DMF following the expectation that a hydrophobic environment promotes the coordination of sulfate to vanadium(III). On the other hand, the spectrum of the aqueous solution is dominated by an intense LMCT band, which is characteristic of a μ-oxo dimer, indicating that most of the coordinated sulfate ion in $[V_2(SO_4)_3(bispicen)_2]$ is displaced by water to generate a hexacoordinate species. The Raman spectrum (Fig. 20B) is typical of the μ-oxo dimer and confirms the conclusion based on the absorption spectrum.

Although an appreciable amount of the heptacoordinate species changes to the hexacoordinate species in aqueous solution, as shown above, the existence of the heptacoordinate species induced by coordination of a bidentate sulfate was proved by comparing the hydrolytic behavior of $[V_2(SO_4)_3(bispicen)_2]$ with that of $[VCl_2(bispicen)]Cl$. Fig. 21 shows the absorbance plots of the LMCT band against the pH of the solution for the sulfato and chloro complexes. Clearly sulfate somewhat suppresses the formation of the V–O–V dimer. This suppression was considered to be a result of sulfate-induced heptacoordination of vanadium(III).

The μ-oxo dimer formation of vanadium(III) complexes with tpen depends more explicitly on ligand anions. As shown in the structure of $[V(III)(SO_4)(tpen)]^+$ complex (Fig. 22), the sulfate ion in this complex again coordinates in a bidentate chelate mode, resulting in the heptacoordinate vanadium(III)

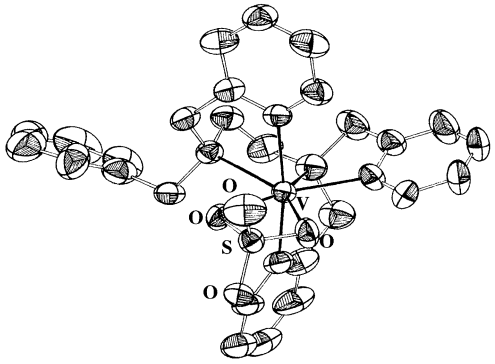

Fig. 22. Structure of $[V(III)(SO_4)(tpen)]^+$ [50].

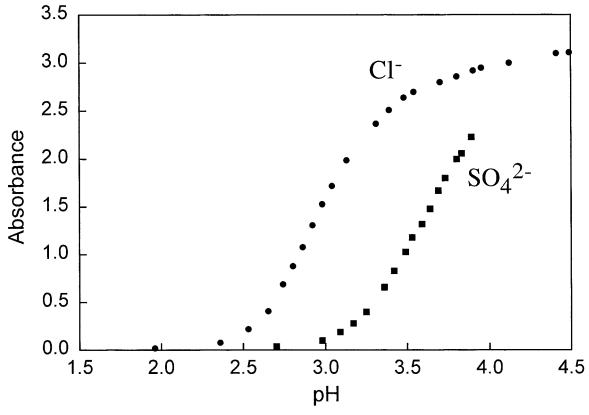

Fig. 21. Plots of the absorbance of the LMCT band against pH of solution for the V(III)–tpen–Cl^- and V(III)–tpen–SO_4^{2-} systems.

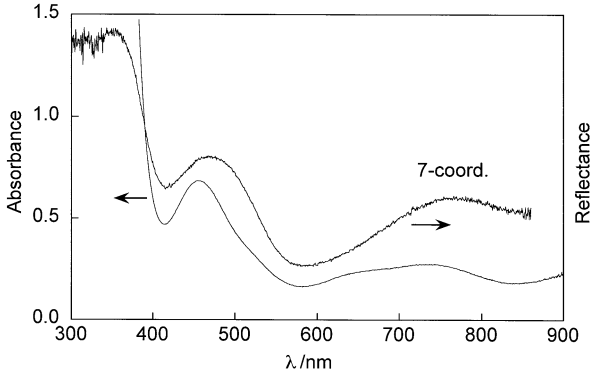

Fig. 23. Diffuse reflectance and absorption (24 mM, pH 2.94) spectra of $[V(III)(SO_4)(tpen)]^+$ [50].

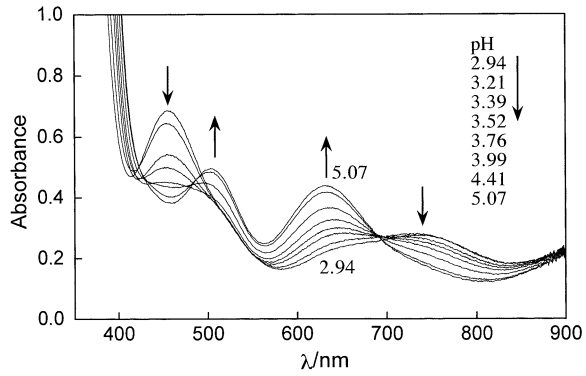

Fig. 24. Absorption spectra of $[V(III)(SO_4)(tpen)]^+$ (25 mM) as function of pH [50].

complex. The diffuse reflectance spectrum in the solid state and the absorption spectrum of aqueous solution are shown in Fig. 23. The band at 760 nm, which is characteristic of heptacoordinate species, was observed for both samples. These observations indicate that the heptacoordinate structure is retained in aqueous solution. Fig. 24 shows the pH dependence of the visible absorption spectrum. Since $[V(III)(SO_4)(tpen)]^+$ does not exhibit the LMCT band at the wavelength characteristic of the V–O–V moiety, it was concluded that the heptacoordinate structure is maintained even in higher pH regions.

Contrary to the above observations, the V(III)–tpen–X^- ($X = Cl^-$ or Br^-) system shows absorption spectra characteristic of a μ-oxo dimer. Namely, a reaction between VX_3 ($X = Cl^-$ or Br^-) and tpen in a 1:1 molar ratio results in a deep-purple color, and the absorption maximum agrees with that of the dinuclear μ-oxo vanadium(III) complex with tpen, $[V_2OBr_4(tpen)]$, which was isolated as a powder [50]. The CT band due to the V–O–V moiety was observed even at pH 1.2 for the halide system, while the CT band was not observed at all for the sulfate system, as stated above. This is considered to be a pronounced effect of sulfate suppressing the formation of the oxo-bridged dinuclear complex.

Recently, the structure of $NaV_3(SO_4)_2(OH)_6$ was solved [51]. In $[V_3(SO_4)_2(OH)_6]^-$, sulfate acts as a tridentate bridging ligand to connect three vanadium(III) ions and hydroxyl groups are shared between two octahedra resulting in a two dimensional net. But it is uncertain if this coordination mode of sulfate is held in solution.

6. Multinuclear vanadium(III) complexes with other bridging modes

Multinuclear vanadium(III) complexes with diverse bridging modes have been structurally characterized. Although some structures may not be relevant to the status of vanadium(III) in the biological system, it is appropriate to present them here in order to show the variety of structures adopted by vanadium(III). Organometallic compounds are, however, not included.

In relation to the dinuclear iron(III) core in hemerythrin, dinuclear vanadium(III) complexes bridged by an oxo (or a hydroxo) group and two carboxylato groups (Scheme 6A) have been extensively studied: $[V(III)_2O(RCOO)_2(Me_3tacn)_2]^{2+}$ (R: CH_3 and Ph) [15,52,53] and $[V(III)_2O(RCOO)_2$(hydridotrispyrazolylborato$)_2]$ (R: various groups) [54,55].

Several trinuclear oxo-centered vanadium(III) complexes with additional di-carboxylato bridges (Scheme 6B) have been prepared and structurally characterized. This type of complex includes $[V(III)_3O(CH_3COO)_6(CH_3COOH)_2(THF)]^+$ [56] and $[V(III)O(RCOO)_6L_3]^+$ (R: various groups; L: pyridine, 4-picoline, 3,5-lutidine) [57].

Di- or multinuclear vanadium(III) complexes with various types of bridging modes, other than the above modes, have been characterized. $[V_2(edt)_4]^{2-}$ (edt: ethane-1,2-dithiolate) contains two bridging edt ligands forming the quadruple $V(\mu\text{-}S)_4V$ unit [58]. In $(NEt_4)_3[V_3Cl_6(edt)_3]$, each of two VCl_3 units coordinate facially to $[V(edt)_3]^{3-}$ from the opposite sides to give a linear trimer [59]. $[V(III)_2\{OC_6H_3(OH)_2\}_2(acac)_4]$ contains di-phenoxo bridges from the pyrogallol ligands [60]. $[V(III)_3S_7(bpy)_3]^+$ and $[V(III)_2O(SPh)_4(Me_2bpy)_2]$ have unique $(\mu_3\text{-}S)(\mu\text{-}S_2)_3$ and $(\mu\text{-}O)(\mu\text{-}SPh)_2$ bridging cores, respectively [61]. $[V(III)_2Cl_6(NNMe_2)_3]^{2-}$ is a triply hydrazide-bridged dinuclear vanadium(III) complex [62]. $[V(III)_2Cl_2(CyN)_4]$ consists of two distorted tetrahedral vanadium centers linked together by two bridging chlorides [63]. The dialkoxo-bridged vanadium(III) dimer has been prepared using a macrocyclic tetraimine Schiff base [64]. In $[V_2Mg_2(\mu_3,\eta^2\text{-}thffo)_2(\mu,\eta^2\text{-}thffo)_4Cl]\cdot 2CH_2Cl_2$ (thffo: 2-tetrahydrofurylmethoxide), the methoxo group of thffo acts as a bridging group [65]. Unique octanuclear vanadium(III) compounds having a cyclic core linked by hydroxo, alkoxo, and carboxylato bridges have been prepared [66]. In $(4,4'\text{-}H_2bpy)[V_2(HPO_4)_4(4,4'\text{-}bpy)_2]$, two vanadium(III) atoms are bridged by two HPO_4 ions and 4,4′-bpy [67]. Squarate-bridged dinuclear vanadium(III) complexes with layered and framework structures have

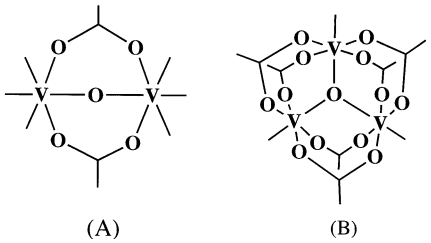

Scheme 6.

been prepared by hydrothermal synthesis [68]. $[V_4O_2(RCOO)_7(bpy)_2]^+$ contains a $[V_4(\mu_3\text{-}O)_2]$ core comprising four vanadium(III) ions with a butterfly disposition and a μ_3-O ion bridging each V_3 wing [69]. $[V_2Cl_7(THF)_2]^-$ contains a $[V_2(\mu\text{-}Cl)_3]$ core [70]. These examples show the diversity in the structures of multinuclear vanadium(III) complexes.

7. Magnetic properties

Although the magnetic behavior of multinuclear vanadium(III) complexes is an important and interesting subject, it is beyond the scope of this review. Thus, we only briefly mention the magnetic properties of dinuclear vanadium(III) complexes. A vanadium(III) ion has a d^2 electron configuration. Magnetic coupling between two vanadium(III) centers of several dinuclear vanadium(III) complexes has been examined. Dinuclear vanadium(III) complexes have diverse coordination geometries as well as bridging modes as shown above, and the magnetic coupling between two vanadium(III) centers in dinuclear vanadium(III) complexes depends strongly on the bridging mode. The spin-exchange coupling constants J for dinuclear vanadium(III) complexes are summarized in Table 1. Spin-exchange coupling changes drastically from a strong ferromagnetic coupling to a strong antiferromagnetic coupling, depending on the bridging modes. It is noteworthy that the spin-exchange coupling of $V_2(\mu\text{-}O)(\mu\text{-}RCOO)_2$ changes from ferromagnetic to antiferromagnetic (spin-switching) upon protonation of the μ-oxo group [53]. Knopp and Wieghardt [53] have first rationalized the above magnetic behavior based on the three spin-exchange pathways (Fig. 25(A)) using the metal-centered orbital model with participation of the oxo ligand

Table 1
Spin-exchange coupling of dinuclear vanadium(III) complexes

Bridging modes	Coordination number	J (cm^{-1})	Ref.
$(O)(RCOO)_2$	6	$>+200$	[15]
(O)	6	+224	[15]
(O)	6	+117	[39]
(RO)(RCOO)	6	+23.7	[45]
(RO)(RCOO)(OH)	7	+14.6	[45]
$(OH)(RCOO)_2$	6	−31.3	[54,55]
$(OH)(RCOO)_2$	6	−35, −36	[53]
$(RO)_2$	7	−8.5	[16]
$(RO)_2$	7	−14.5	[27]
$(RO)_2$	7	−20, −25	[64]
$(RO)_2$	7	−25.4, −35.2	[45]
$(RO)_2$	6	−36.9	[43]
$(PhO)_2$	6	−44.8	[60]
$(Cl)_3$	6	−48.1	[70]
$(O)(SPh)_2$	6	−355	[61]
$(SRS)_2$	6	−419	[59]

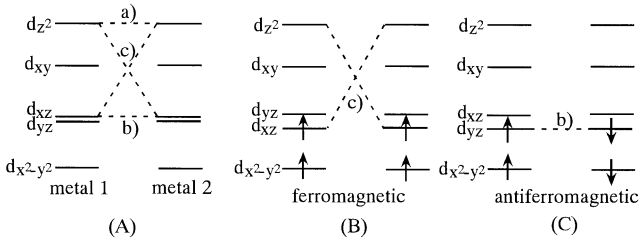

Fig. 25. (A) Schematic representation of the energetic order of d orbitals and symmetry-allowed spin exchange coupling pathway in M(μ-O)(μ-carboxylato)$_2$M complexes. (B) Schematic representation of spin exchange pathway in V(III)(μ-O)(μ-carboxylato)$_2$V(III). (C) Schematic representation of spin exchange pathway in V(III)(μ-OH)(μ-carboxylato)$_2$V(III). (Figures were reproduced from Ref. [53].)

p orbitals: pathway (a), interaction between two d_{z^2} orbitals of both metal ions with a filled p orbital of the oxo ligand; pathway (b), interaction between two d_{yz} orbitals with a p orbital of the oxo ligand; pathway (c), interaction between a d_{xz} orbital at metal 1, a p orbital of the oxo ligand, and a d_{z_2} orbital of metal 2 (the "crossed pathway"). The sign of the intramolecular spin-exchange coupling constant J results from the sum of antiferromagnetic and ferromagnetic contributions; i.e. $J = J_{AF} + J_F$. The actual magnitude of J_{AF} and J_F are dependent on the respective orbital overlap, on the nature of the metal ion, and on the actual M–O bond length. The pathway (c) is especially sensitive to the M–O bond length. They explained the spin-switching of V2(μ-O)(μ-RCOO)$_2$ by protonation of the oxo-bridge on the ground of the above view. They suggested that the approximate degeneracy of the d_{yz} and d_{xz} orbitals is lifted due to a lower symmetry of the dinuclear vanadium(III) complexes or as a consequence of spin-orbit coupling. If the d_{xz} orbitals are energetically more favorable than the d_{yz} orbitals, the only available spin-exchange pathway would be c, which leads to a strong ferromagnetic coupling (Fig. 25(B)). Protonation of the oxo bridge, which weakens the V(III)–O bond, may reverse the energetic order of the d_{yz} and d_{xz} orbitals, with d_{yz} being more favorable. The pathway (b) then is the only available spin-exchange pathway, leading to an antiferromagnetic coupling. Such a mechanism, how-

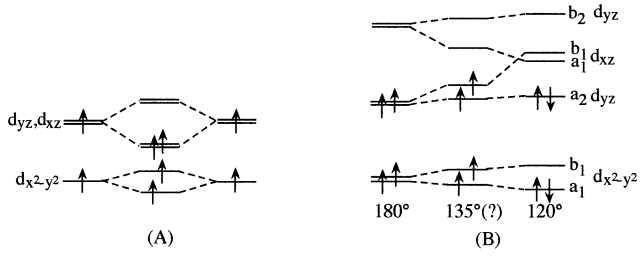

Fig. 26. (A) Qualitative MO diagram for a linear V(III)–O–V(III) dimer [71]. (B) Qualitative MO diagram depending on V–O–V angle for oxo-bridged V(III) dimers [55]. (Figures were modified from the original ones.)

ever, cannot be valid for a ferromagnetically-coupled linear V(III)–O–V(III) system, since the "crossed pathway (c)" does not exist by symmetry. Hotzelmann et al. [71] have proposed the MO scheme (Fig. 26(A)) to rationalize the ferromagnetic coupling of linear V(III)–O–V(III) complexes. Bond et al. [55] have also applied the MO scheme to rationalize the spin-switching dependence on the V–O–V angle of the oxo-bridged dinuclear vanadium(III) complexes (Fig. 26(B)). They postulated that the ferromagnetic coupling of the linear V(III)–O–V(III) dimer should persist as the V–O–V angle decreases until the gain in orbital energy obtained through spin-pairing exceeds the spin-pairing energy itself, and the exchange coupling should switch from ferromagnetic to antiferromagnetic at this point. They have indicated that strong ferromagnetic coupling persists through the V–O–V angle range 180–130° in the μ-oxo vanadium(III) complexes, but that the μ-hydroxo vanadium(III) complexes become less antiferromagnetic as the V–O(H)–V angle increases from 120°. Ab initio calculations of the magnetic exchange coupling in linear oxo-bridged dinuclear metal complexes have been performed in detail [72].

8. Summary

The stereochemistry of vanadium(III) complexes flexibly changes depending on the ligand structure and functional groups. For example, although the heptacoordinate structure is not so common for the first low-transition-metal complexes, vanadium(III) complexes with a multidentate aminopolycarboxylate ligand that only gives five-membered chelate rings usually adopt the heptacoordinate structure. Three possible geometries for the heptacoordinate structure, a pentagonal bipyramid, a capped octahedron, and a capped trigonal prism, are all realized for vanadium(III) complexes. This structural flexibility may, at least partly, come from a relatively small ligand field stabilization energy of d^2 system. Substitution of carboxylate group(s) of aminopolycarboxylate ligand with stronger pyridylmethyl group(s) results in a hexacoordinate structure regardless of the chelate ring size.

In dinuclear vanadium(III) complexes, not only the coordination number but also the bridging mode changes depending on the structure and functional groups of the ancillary ligands. The magnetic exchange coupling also dramatically changes from strong antiferromagnetic coupling to strong ferromagnetic coupling depending on the bridging mode. Spin-switching by protonation of the oxo group was observed for (μ-O)bis(μ-carblylato) and (μ-O)bis(μ-phosphato) vanadium(III) complexes. The change in the V–O–V angle is considered to be responsible for this phenomenon.

Sulfate tends to coordinate to vanadium(III) in a bidentate fashion (bidentate chelate or bidentate bridge). Sulfate coordination suppresses the formation of the oxo-bridged dimer due to base hydrolysis for some vanadium(III) complexes, probably due to the heptacoordination induced by the bidentate sulfate. Information on the coordination mode of sulfate will eventually assist us in gaining further insight into the puzzling role of sulfate in ascidian blood cells.

Accumulation and storage of vanadium(III) ions by ascidians is still a subject left unsolved. We believe that fundamental studies on the coordination chemistry of vanadium(III) would shed new light on this fascinating problem.

Acknowledgements

K.K. thanks the Ministry of Education, Science, Sports and Culture and the Izumi Science and Technology Foundation for funding this work.

References

[1] M. Henze, Hoppe-Seyler's Z. Physiol. Chem. 72 (1911) 494.
[2] (a) H. Michibata, H. Hirose, K. Sugiyama, Y. Ookubo, K. Kanamori, Biol. Bull. 179 (1990) 140;
(b) H. Michibata, T. Uyama, K. Kanamori, The accumulation mechanism of vanadium in ascidians, in: A.S. Tracey, D.C. Crans (Eds.), Vanadium Compounds: Chemistry, Biochemistry, and Therapeutic Applications, ACS Symposium Series 711, American Chemical Society, Washington, DC, 1998, pp. 248–258.;
(c) H. Michibata, K. Kanamori, Selective accumulation of vanadium by ascidians from sea water, in: J.O. Nriagu (Ed.), Vanadium in the Environment, Advances in Environmental Science and Technology, vol. 30, Wiley, New York, 1998, pp. 217–249.
[3] (a) B.J.S. Pirie, M.V. Bell, J. Exp. Mar. Biol. Ecol. 74 (1984) 187;
(b) P. Frank, R.M.K. Carlson, K.O. Hodgson, Inorg. Chem. 25 (1986) 470;
(c) P. Frank, B. Hedman, R.M.K. Carlson, T.A. Tyson, A.L. Roe, K.O. Hodgson, Biochemistry 26 (1987) 4975;
(d) P. Frank, R.M.K. Carlson, K.O. Hodgson, Inorg. Chem. 27 (1988) 118.
[4] T. Ishii, I. Nakai, C. Numako, K. Okoshi, T. Otake, Naturwissenshaften 80 (1993) 268.
[5] M.J. Smith, D.E. Ryan, K. Nakanishi, P. Frank, K.O. Hodgson, Vanadium in ascidians and the chemistry of tunichromes, in: H. Sigel, A. Sigel (Eds.), Metal Ions in Biological Systems, Vol. 31, Vanadium and Its Role in Life, Dekker, New York, 1995, pp. 423–490.
[6] T. Ishii, Characterization of vanadium in the fan worm, in: J.O. Nriagu (Ed.), Vanadium in the Environment, Advances in Environmental Science and Technology, vol. 30, Wiley, New York, 1998, pp. 199–216.
[7] J.J.R. Fraústo da Silva, R.J.P. Williams, The Biological Chemistry of the Elements—The Inorganic Chemistry of Life, Oxford University Press, New York, 1997.
[8] E. Boeri, A. Ehrenberg, Arch. Biochem. Biophys. 50 (1954) 404.
[9] L. Pajdowski, Roczniki Chem. 37 (1963) 1351.
[10] T.W. Newton, F.B. Baker, Inorg. Chem. 3 (1964) 569.

[11] P. Chandrasekhar, P. Bird, Inorg. Chem. 23 (1984) 3677.
[12] J.K. Money, K. Folting, J.C. Huffman, G. Christou, Inorg. Chem. 26 (1987) 944.
[13] S.G. Brand, N. Edelstein, C.J. Hawkins, G. Shalimoff, M.R. Snow, E.R.T. Tiekink, Inorg. Chem. 29 (1990) 434.
[14] Y. Zhang, R.H. Holm, Inorg. Chem. 29 (1990) 911.
[15] P. Knopp, K. Wieghardt, B. Nuber, J. Weiss, W.S. Sheldrick, Inorg. Chem. 29 (1990) 363.
[16] T.K. Shepherd, W.E. Hatfield, D. Ghosh, C.D. Stout, F.J. Kristine, J.R. Ruble, J. Am. Chem. Soc. 103 (1981) 5511.
[17] K. Kanamori, Y. Ookubo, K. Ino, K. Kawai, H. Michibata, Inorg. Chem. 30 (1991) 3832.
[18] R.S. Czernuszewicz, J.E. Sheats, T.G. Spiro, Inorg. Chem. 26 (1987) 2063.
[19] S.E. Lincoln, T.M. Loehr, Inorg. Chem. 29 (1990) 1907.
[20] R.S. Czernuszewicz, G. Spiro, IR, Raman, and resonance Raman spectroscopy, in: E.I. Solomon, A.B.P. Lever (Eds.), Inorganic Electronic Structure and Spectroscopy, Vol. 1: Methodology, Wiley, New York, 1999, pp. 353–441.
[21] T.K. Myser, R.E. Shepherd, Inorg. Chem. 26 (1987) 1544.
[22] F.J. Kristine, R.E. Shepherd, J. Am. Chem. Soc. 99 (1977) 6562.
[23] K. Kanamori, K. Ino, H. Maeda, K. Miyazaki, M. Fukagawa, J. Kumada, T. Eguchi, K. Okamoto, Inorg. Chem. 33 (1994) 5547.
[24] M. Shimoi, Y. Saito, H. Ogino, Chem. Lett. (1989) 1675.
[25] K. Kanamori, J. Kumada, M. Yamamoto, T. Okayasu, K. Okamoto, Bull. Chem. Soc. Jpn. 68 (1995) 3445.
[26] K. Okamoto, J. Hidaka, M. Fukagawa, K. Kanamori, Acta Crystallogr. C48 (1992) 1025.
[27] J.C. Robles, Y. Matsuzaka, S. Inomata, M. Shimoi, W. Mori, H. Ogino, Inorg. Chem. 32 (1993) 13.
[28] M. Shimoi, S. Miyasato, H. Ogino, Bull. Chem. Soc. Jpn. 64 (1991) 2549.
[29] J.A. Jensen, G.S. Girolami, Inorg. Chem. 28 (1989) 2114.
[30] K. Kanamori, A. Kyoto, K. Fujimoto, K. Nagata, H. Suzuki, K. Okamoto, Bull. Chem. Soc. Jpn. 74 (2001) 2113.
[31] K. Kanamori, E. Kameda, T. Kabetani, T. Suemoto, K. Okamoto, S. Kaizaki, Bull. Chem. Soc. Jpn. 68 (1995) 2581.
[32] K. Kanamori, M. Teraoka, H. Maeda, K. Okamoto, Chem. Lett. (1993) 1731.
[33] R.S. Czernuszewicz, Q. Yan, M.R. Bond, C.J. Carrano, Inorg. Chem. 33 (1994) 6116.
[34] K. Bukietynska, Z. Karwecka, H. Podsiadly, Polyhedron 16 (1997) 2613.
[35] J. Sanders-Loehr, W.D. Wheeler, A.K. Shiemko, B.A. Averill, T.M. Loehr, J. Am. Chem. Soc. 111 (1989) 8084.
[36] A.Y. Hirakawa, M. Tsuboi, Science 188 (1975) 359.
[37] (a) T. Otieno, M.R. Bond, L.M. Mokry, R.B. Walter, C.J. Carrano, Chem. Commun. (1996) 37;
(b) S.J. Heater, M.W. Carrano, D. Rains, R.B. Walter, D. Ji, Q. Yan, R.S. Czernuszewicz, C.J. Carrano, Inorg. Chem. 39 (2000) 3881.
[38] Th. Sichla, R. Niewa, U. Zachweja, R. Eßmann, H. Jacob, Z. Anorg. Allg. Chem. 622 (1996) 2074.
[39] C.M. Grant, B.J. Stamper, M.J. Knapp, K. Folting, J.C. Huffman, D.N. Hendrickson, G. Christou, J. Chem. Soc. Dalton Trans. (1999) 3399.
[40] R.C. Holz, T.E. Elgren, L.L. Pearce, J.H. Zhang, C.J. O'connor, L. Que, Jr., Inorg. Chem. 32 (1993) 5844.
[41] R.C. Reem, J.M. McCormick, D.E. Richardson, F.J. Devlin, P.J. Stephens, R.L. Musselman, E.I. Solomon, J. Am. Chem. Soc. 111 (1989) 4688.
[42] A.B.P. Lever, E.S. Dodsworth, Electrochemistry, charge transfer spectroscopy, and electronic structure, in: E.I. Solomon, A.B.P. Lever (Eds.), Inorganic Electronic Structure and Spectroscopy: Application and Case Studies, vol. 2, Wiley, New York, 1999, pp. 227–289.
[43] K. Kanamori, K. Ishida, K. Fujimoto, T. Kuwai, K. Okamoto, Bull. Chem. Soc. Jpn. 74 (2001) 2377.
[44] K. Kanamori, K. Yamamoto, K. Okamoto, Chem. Lett. (1993) 1253.
[45] K. Kanamori, K. Yamamoto, T. Okayasu, N. Matsui, K. Okamoto, W. Mori, Bull. Chem. Soc. Jpn. 70 (1997) 3031.
[46] K. Kanamori, T. Okayasu, K. Okamoto, Chem. Lett. (1995) 105.
[47] K. Kanamori, manuscript in preparation.
[48] P. Frank, B. Hedman, R.M.K. Carlson, K.O. Hodgson, Inorg. Chem. 33 (1994) 3794.
[49] K. Kanamori, N. Kunita, K. Okamoto, J. Hidaka, Bull. Chem. Soc. Jpn. 66 (1993) 2574.
[50] K. Kanamori, E. Kameda, K. Okamoto, Bull. Chem. Soc. Jpn. 69 (1996) 2901.
[51] A. Dobley, P.Y. Zavalij, M.S. Whittingham, Acta Crystallogr. C56 (2000) 1294.
[52] M. Köppen, G. Fresen, K. Wieghardt, R.M. Llusar, B. Nuber, J. Weiss, Inorg. Chem. 27 (1988) 721.
[53] P. Knopp, K. Wieghardt, Inorg. Chem. 30 (1991) 4061.
[54] C.J. Carrano, R. Verstague, M.R. Bond, Inorg. Chem. 32 (1993) 3589.
[55] M.R. Bond, R.S. Czernuszewicz, B.C. Dave, Q. Yan, M. Mohan, R. Verastegue, C.J. Carrano, Inorg. Chem. 34 (1995) 5857.
[56] F.A. Cotton, G.E. Lewis, G.M. Mott, Inorg. Chem. 21 (1982) 3316.
[57] S.L. Castro, W.E. Streib, J. Sun, G. Christou, Inorg. Chem. 35 (1996) 4462.
[58] J.R. Dorfman, R.H. Holm, Inorg. Chem. 22 (1983) 3179.
[59] J.R. Rambo, S.L. Castro, K. Folting, S.L. Bartley, R.A. Heintz, G. Christou, Inorg. Chem. 35 (1996) 6844.
[60] S. Lee, K. Nakanishi, M.Y. Chiang, R.B. Frankel, K. Spartallian, J. Chem. Soc. Chem. Commun. (1988) 785.
[61] (a) N.S. Dean, K. Folting, E. Lobkovsky, G. Christou, Angew. Chem. Int. Ed. Engl. 32 (1993) 594;
(b) N.S. Dean, S.L. Bartley, W.E. Streib, E.B. Lobkovsky, G. Christou, Inorg. Chem. 34 (1995) 1608.
[62] C. Le Floc'h, R.A. Henderson, P.B. Hitchcock, D.L. Hughes, Z. Janas, R.L. Richards, P. Sobota, S. Szafert, J. Chem. Soc. Dalton Trans. (1996) 2755.
[63] P. Berno, M. Moore, R. Minhas, S. Gambarotta, Can. J. Chem. 74 (1996) 1930.
[64] P.E. Kruger, B. Moubaraki, K.S. Murray, J. Chem. Soc. Dalton Trans. (1996) 1223.
[65] Z. Janas, P. Sobota, M. Klimowicz, S. Szafert, K. Szczegot, L.B. Jerzykiewicz, J. Chem. Soc. Dalton Trans. (1997) 3897.
[66] H. Kumagai, S. Kitagawa, Chem. Lett. (1996) 471.
[67] C.-H. Huang, L.-H. Huang, K.-H. Lii, Inorg. Chem. 40 (2001) 2625.
[68] K.-J. Lin, K.-H. Lii, Angew. Chem. Int. Ed. Engl. 36 (1977) 2076.
[69] S.L. Castro, Z. Sun, C.M. Grant, J.C. Bollinger, D.N. Hendrickson, G. Christou, J. Am. Chem. Soc. 120 (1998) 2365.
[70] J.R. Rambo, S.L. Bartley, W.E. Streib, G. Christou, J. Chem. Soc. Dalton Trans. (1994) 1813.
[71] R. Hotzelmann, K. Wieghardt, U. Flörke, H.-J. Haupt, D.C. Weatherburn, J. Bonvoisin, G. Blondin, J.-J. Girerd, J. Am. Chem. Soc. 114 (1992) 1681.
[72] K. Fink, R. Fink, V. Staemmier, Inorg. Chem. 33 (1994) 6219.